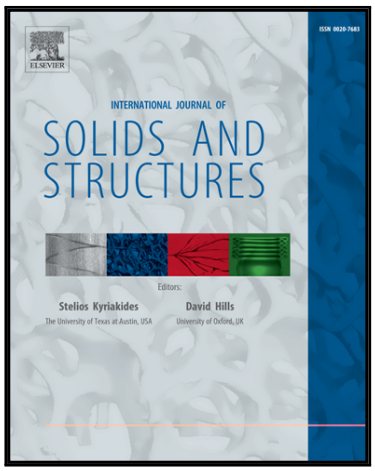

Fabric Response to Strain Probing in Granular Materials: Two-dimensional, Isotropic Systems

Mehdi Pouragha, Niels P. Kruyt, Richard Wan

PII: S0020-7683(18)30338-X
DOI: https://doi.org/10.1016/j.ijsolstr.2018.08.020
Reference: SAS 10094

To appear in: *International Journal of Solids and Structures*

Received date: 2 March 2018
Revised date: 2 August 2018
Accepted date: 21 August 2018

Please cite this article as: Mehdi Pouragha, Niels P. Kruyt, Richard Wan, Fabric Response to Strain Probing in Granular Materials: Two-dimensional, Isotropic Systems, *International Journal of Solids and Structures* (2018), doi: https://doi.org/10.1016/j.ijsolstr.2018.08.020

Fabric Response to Strain Probing in Granular Materials: Two-dimensional, Isotropic Systems

Mehdi Pouragha[a,*], Niels P. Kruyt[b], Richard Wan[a]

[a] *Civil Engineering Department, University of Calgary, Canada*
[b] *Department of Mechanical Engineering, University of Twente, The Netherlands*

Abstract

The stress-deformation behaviour of granular media is known to be directly linked to details of the underlying microstructure of contacts, or fabric. The notion of contact fabric and its role in defining stress and strain motivate the present study to explore the evolution of fabric in response to *small* strain probes applied to initially isotropic granular assemblies of varying void ratios and coordination numbers. Two-dimensional Discrete Element Method simulations demonstrate that the fabric response strongly depends on the strain probe direction, despite the stress response being "pseudo-elastic" and incrementally linear. This direction dependence leads to a so-called incrementally nonlinear property of fabric changes in the small deformation regime, a constitutive characteristic that can serve as a precursor signalling the more intricate, elasto-plastic behaviour of anisotropic granular materials. The present study provides a systematic analysis based on a representation theorem for two-dimensional isotropic functions to characterize fabric changes during strain probing. Contact reorientation is found to be negligible vis-à-vis contact gains and losses which are prevalent in compressive and extension strain probes, respectively. In the end, it is the subtle evolution of gained and lost contacts in various strain probes that helps us elucidate the nature of important fabric changes in the pseudo-elastic regime of granular media.

*Corresponding author
Email address: mpouragh@ucalgary.ca (Mehdi Pouragha)

Keywords: Granular materials, Micromechanics, Fabric, Strain probes

1. Introduction

The micromechanical study of granular material behaviour identifies and exploits connections between their various characteristics at the macroscopic-continuum and microscopic-particle scales with interparticle contacts as the main focus. For instance, micromechanical descriptions of stress [33, 54, 16, 45, 5] and strain [24, 7], and dilatancy in particular [9, 53, 26, 28], show the importance of the internal microstructural arrangement of contacts to macroscopic behaviour. Such studies suggest that a detailed understanding of the evolution of the contact microstructure during mechanical loading is an important aspect of micromechanics-based constitutive modelling of granular materials [50, 31, 55, 32, 18].

The structure of the interparticle contact network is often characterized by a so-called contact fabric tensor [35, 48] which describes the density of contacts, as well as their directional distribution, in terms of a symmetric, second (or sometimes higher) order tensor. Such a tensorial description is often equivalent to a harmonic representation of the distribution of all contact orientations [21, 22]. Apart from its principal directions, such a symmetric second-order fabric tensor is characterized by the coordination number, defined as the average number of contacts per particle, and the fabric anisotropy which quantifies the deviation of the fabric tensor from isotropy.

The statistical analysis of the micromechanical expression for the average stress tensor [16, 33, 54], in terms of interparticle contact forces and the branch vectors that connect centroids of particles that are in contact, by Rothenburg and coworkers [45, 47], as well as the more recent studies on particle kinematics [23, 52, 40, 26], have connected stress and strain to coordination number and fabric anisotropy, thus leading to stress-strain-fabric relations for different stages of loading [43, 42]. In the limit, at the critical state, the fabric tensor is known to possess specific features [32, 20, 27, 39], which further emphasizes the

importance of contact fabric as a state variable in the constitutive modelling of granular materials.

Considering the broad role of contact fabric, it is crucial to have a good understanding of its evolution during loading history in any micromechanical analysis. In fact, this question has been addressed in previous studies, see for instance a thorough review given in [23]. In general, these previous studies can be categorized into two groups, based on whether fabric evolution is related to stress [36] or to strain [10, 44, 46, 49, 23] increment.

More recent studies have distinguished the different mechanisms by which the fabric tensor can evolve during deformation [23, 41]. These mechanisms are: contact gain, contact loss and contact reorientation. Accordingly, Pouragha and Wan [41] have developed an analytical method in which the contact loss mechanism is assumed to be controlled by changes in the average interparticle force and stress, while the contact gain mechanism is seen to be controlled by deformations at the contact level arising from the strain increment.

Nonetheless, such previous studies mentioned above mostly consider fabric evolution under common *monotonic* loading conditions, such as in biaxial, triaxial, or isochoric tests. Certainly, this restricts the generality of such studies since the elasto-plastic response of granular materials is incremental in nature and generally depends upon the direction of loading [13, 14, 34, 51]. This direction dependence, or incremental nonlinearity, of the incremental response has been studied in detail by considering proportional *stress (or strain) probing* [19, 8, 11], where vertical and horizontal stress (or strain) increments in varying ratios are applied to the granular assembly, while the magnitude of the applied loading increment is kept constant.

As it stands, the directional dependence of the *fabric response* to strain probing has not been considered in the recent archival literature. In a first step to address this interesting topic, the direction dependence of the fabric response is investigated herein for isotropic, two-dimensional granular assemblies with different initial coordination numbers. The scope of the study has been limited to isotropic systems, also because the previous results in [23] and [41] showed

a very rapid evolution of coordination number with shear strain for initially very dense samples, which is an intriguing, unexpected behaviour in the small deformation regime.

Discrete Element Method (DEM for short) simulations have been performed on isotropic, two-dimensional granular assemblies, and the various contributions to the evolution of the fabric tensor due to the contact loss, gain, and reorientation mechanisms have been investigated. The incremental stress-strain relationship has been found to be "pseudo-elastic" which denotes an incrementally linear relation without significant plastic dissipation. As defined here, the "pseudo-elasticity" concept differs from conventional elasticity in that it does not require reversibility in every aspect. One of the main findings of this study is that even though the stress response in isotropic conditions is pseudo-elastic (and linear in the applied strain increment), the fabric response shows a clear *incrementally nonlinear* response reflected in the dependence on the direction of the applied strain increment. Hence, even for isotropic assemblies, the fabric response shows precursors of an elasto-plastic stress-strain response, reflected as the dependency of the stress response on the direction of loading.

The paper is organized in the following manner. After a brief description in Section 2 of the basics of the micromechanics of granular materials and the employed strain probing method, the DEM simulations are described in Section 3 and simulation results are subsequently presented in Section 4. The paper concludes with the main findings and suggestions for future extensions in Section 5.

2. Micromechanics

The interparticle contact arrangement, i.e. the microstructure, of a granular assembly is often characterized by a second-order fabric tensor $\boldsymbol{F}$ that describes the density and the directional distribution of contact normals as [35, 48, 22]:

$$F_{ij} = \frac{2}{N_p} \sum_{c \in \mathbb{C}} n_i^c \, n_j^c \tag{1}$$

where N_p is the number of particles (excluding rattlers, i.e. particles with fewer than two contacts), $\mathbb{C}$ is the set of all contacts in the region under consideration, and $\boldsymbol{n}^c$ is the contact normal vector at contact c. Alternatively to the contact fabric considered here, the internal fabric of granular materials has also been characterized based on a void network, see [48, 6, 29, 30].

Coordination number, Z, denoting the average number of contacts per particle, and an anisotropy measure, A, are defined, for the two dimensional case considered here, in terms of the principal values F_1 and F_2 of the fabric tensor $\boldsymbol{F}$ by

$$Z = \frac{2N_c}{N_p} = \mathrm{tr}(\boldsymbol{F}) = F_1 + F_2, \quad A = F_1 - F_2 \tag{2}$$

with N_c being the total number of contacts. The fabric parameters A and Z are related to the common fabric anisotropy parameter, a_c, defined in [45], by $2A = a_c\, Z$.

As the contact structure evolves during loading, the fabric tensor can change due to three different mechanisms [23]: contact loss, contact gain, and contact reorientation. In tracing the evolution of the contact structure, the sets of lost and gained contacts are denoted by $\Delta\mathbb{C}^l$ and $\Delta\mathbb{C}^g$ respectively, while $\mathbb{C}^r$ is the set of persisting contacts. These sets are formally defined, in terms of the sets of all contacts in an initial and a final stage, $\mathbb{C}^{\mathrm{init}}$ and $\mathbb{C}^{\mathrm{final}}$, by [23]:

$$\begin{aligned} \Delta\mathbb{C}^l &= \mathbb{C}^{\mathrm{init}} - \mathbb{C}^{\mathrm{final}} \\ \Delta\mathbb{C}^g &= \mathbb{C}^{\mathrm{final}} - \mathbb{C}^{\mathrm{init}} \\ \mathbb{C}^r &= \mathbb{C}^{\mathrm{init}} \cap \mathbb{C}^{\mathrm{final}} \end{aligned} \tag{3}$$

where $A \cap B$ and $A - B$ denote the intersection and the set difference (or relative complement), respectively, of arbitrary sets A and B.

Based on the definition of the fabric tensor $\boldsymbol{F}$ given in Eq. 1 and the contact sets $\Delta\mathbb{C}^l$, $\Delta\mathbb{C}^g$, and $\mathbb{C}^r$ in Eq. 3, the contribution of each mechanism (contact loss, gain, and reorientation) to the fabric change $\Delta\boldsymbol{F}$ can then be expressed

by:

$$\begin{aligned}\Delta F_{ij} &= \frac{2}{N_p}\Big(\sum_{c\in\mathbb{C}^{\text{final}}} n_i^c\, n_j^c - \sum_{c\in\mathbb{C}^{\text{init}}} n_i^c\, n_j^c\Big) \\ &= \frac{2}{N_p}\sum_{c\in\Delta\mathbb{C}^g} n_i^c\, n_j^c - \frac{2}{N_p}\sum_{c\in\Delta\mathbb{C}^l} n_i^c\, n_j^c + \frac{2}{N_p}\sum_{c\in\mathbb{C}^r}\Delta(n_i^c\, n_j^c) \qquad (4)\\ &= \quad \Delta F_{ij}^g \quad - \quad \Delta F_{ij}^l \quad + \quad \Delta F_{ij}^r\end{aligned}$$

where it has been assumed that N_p, the number of particles excluding rattlers, is constant. The value of N_p may actually evolve as the number of rattlers may change due to contact gain/loss. However, the effect is infinitesimal for the size of the incremental probing considered here.

The change in fabric tensors associated with contact loss and gain, defined in Eq. 4, can also be visualized in terms of the change in orientational distributions of the number of contacts due to each mechanism. The orientation of a contact c is the orientation of its contact normal vector, $\boldsymbol{n}^c$, and polar histograms can be used to illustrate the change in the number of contacts for each orientation due to contact loss and gain. Following the analysis in [22], the orientational distribution of contact number changes due to contact loss and contact gain can be readily expressed in terms of their associated fabric changes in Eq. 4 as:

$$\Delta N^m(\boldsymbol{n}) = \frac{\Delta N^{m,\text{tot}}}{4\pi}\left(\frac{4}{\text{tr}(\Delta \boldsymbol{F}^m)}\Delta F_{ij}^m - \delta_{ij}\right) n_i n_j, \quad m = l,\, g \qquad (5)$$

where $\Delta N^m(\boldsymbol{n})$, and $\Delta N^{m,\text{tot}}$ are the change in the number of contacts along direction $\boldsymbol{n}$ and the change in the total number of contacts due to mechanism m, respectively; index m (a mnemonic for mechanism) here refers to the contact loss (l), gain (g) mechanisms. While not considered in this study, similar relations, with minor modifications, can also be obtained for the fabric change due to contact reorientation.

Although previous studies such as [23, 41] have provided insights as to how the fabric tensor changes due to these mechanisms, nevertheless, the scope of these studies has been limited to a single loading monotonic (stress or strain) path. In order to broaden the scope towards a more general framework, the current study investigates the evolution of the fabric tensor in response to dif-

ferent proportional loading paths by applying strain probes. As a first step towards the study of the more complex anisotropic systems, the current work is restricted to isotropic initial samples.

As illustrated schematically in Fig. 1, the strain probing analysis method involves applying small vertical and horizontal strain increments, $\Delta\varepsilon_{yy}$ and $\Delta\varepsilon_{xx}$, to a granular assembly bounded by four walls, and varying the ratio $\Delta\varepsilon_{yy}/\Delta\varepsilon_{xx}$ such that the magnitude of the total strain increment $||\Delta\varepsilon|| \equiv \sqrt{\Delta\varepsilon_{yy}^2 + \Delta\varepsilon_{xx}^2}$ is the same for all strain probes. The stresses on the horizontal and vertical walls and the internal fabric changes are then evaluated as the response. The sign convention adopted here for strain and stress is that tensile strains and stresses are considered to be positive, while compression is considered negative.

The definition of the strain-probe direction α is also given in Fig. 1. It should be noticed that the parameter α is a measure of strain increment ratios, and hence does not refer to geometrical angles in space. Also, in Fig. 1, and throughout this study, the following characteristic directions α of the strain probes are indicated for easy referencing: isotropic extension ($\alpha = 45°$), isotropic compression ($\alpha = 225°$), pure shear ($\alpha = 135°$ and $\alpha = 315°$), uniaxial extension in y-direction ($\alpha = 90°$), uniaxial compression in x-direction ($\alpha = 180°$).

Assuming that the applied strain increments are infinitesimally small, the responses can be assumed to be linear with respect to the magnitude of the strain increment $||\Delta\varepsilon||$, sufficient for the changes to reflect a constant representative rate. For the isotropic initial samples and strain probes considered in the current study, the incremental changes in stress and fabric are coaxial with incremental strains for which $\Delta\varepsilon_{yy}$ and $\Delta\varepsilon_{xx}$ are herein principal values.

Such a strain probing procedure involves applying only normal principal strains, which, for isotropic systems, does not limit the generality of the observations. For initially anisotropic cases, such an incremental strain probing can be extended to strain increments with shear terms such that the principal directions of the applied probes and the responses are no longer coaxial with the current stress. In these cases, the applied probes and the response envelopes

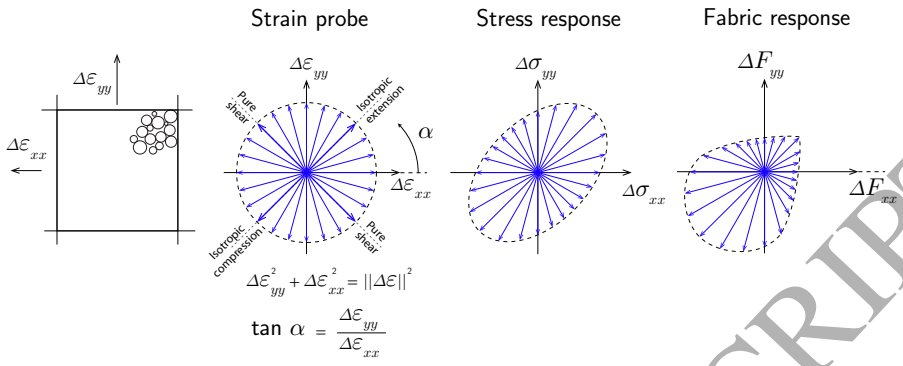

Figure 1: Schematics of strain probe, stress response and fabric response.

should be visualized in 3D to include the three variables characterizing the stress and strain increments.

In general, the fabric response tensor $\Delta\boldsymbol{F}$ shown schematically in Fig. 1 (right) can be assumed to be a function of the strain increment tensor, $\Delta\boldsymbol{\varepsilon}$, imposed by the probes:

$$\Delta\boldsymbol{F} = \boldsymbol{h}(\Delta\boldsymbol{\varepsilon}) \tag{6}$$

In this particular study, note that no additional dependence of the fabric change on plastic strain needs to be considered, as the stress response will be shown to be pseudo-elastic in Section 4, where it will also be demonstrated that the response due to a strain probe is linear with respect to its magnitude $||\Delta\varepsilon||$. Therefore, Eq. 6 is positively homogeneous of degree one in $\Delta\boldsymbol{\varepsilon}$, and hence it can also be expressed in terms of the fabric rate of change scaled to strain probe size as:

$$\Delta F_{ij}^{*} = \frac{\Delta F_{ij}}{||\Delta\boldsymbol{\varepsilon}||} = h_{ij}(\Delta\boldsymbol{\varepsilon}^{*}), \quad \Delta\varepsilon_{ij}^{*} = \frac{\Delta\varepsilon_{ij}}{||\Delta\boldsymbol{\varepsilon}||} = \begin{bmatrix} \cos\alpha & 0 \\ 0 & \sin\alpha \end{bmatrix} \tag{7}$$

where $\Delta\varepsilon_{ij}^{*}$ is the *normalized* strain increment that is determined by the direction of the strain probe defined by the angle α in the incremental strain space.

Based on a representation theorem for the functional dependence of a second-order tensor on another second-order tensor for isotropic two-dimensional ma-

terials [15], the relationship in Eq. 7 can be expressed as:

$$\Delta F_{ij}^{*} = h_{ij}(\Delta\boldsymbol{\varepsilon}^{*}) = \psi_1 \delta_{ij} + \psi_2 \Delta\varepsilon_{ij}^{*} \tag{8}$$

with ψ_1 and ψ_2 being coefficients that depend on the material state (e.g. the initial coordination number, Z_0) and are also functions of the invariants of the *normalized* strain increment tensor $\Delta\boldsymbol{\varepsilon}^{*}$. In the two-dimensional case, the invariants involved are the trace, $\mathrm{tr}(\Delta\boldsymbol{\varepsilon}^{*})$, and determinant, $\det(\Delta\boldsymbol{\varepsilon}^{*})$, which can be expressed as:

$$\begin{aligned} \mathrm{tr}(\Delta\boldsymbol{\varepsilon}^{*}) &= \cos\alpha + \sin\alpha \\ \det(\Delta\boldsymbol{\varepsilon}^{*}) &= \cos\alpha \, \sin\alpha \end{aligned} \tag{9}$$

Recalling that $\Delta\boldsymbol{\varepsilon}^{*}$ is a function of solely the strain probe *direction*, the expression in Eq. 8 can be conveniently used to fit the variation of the observed fabric change $\Delta\boldsymbol{F}^{*}$ with probe direction α, as will be shown in Section 4. Although not discussed in this study, the form of the functions given in Eqs. 6 to 9 can also be used to describe the stress response to the strain probes.

It should be noted that, in its general form, the fabric evolution expression in Eq. 8 is obviously incrementally nonlinear (not to be confused with the linearity of the response in the magnitude of the strain increment $||\Delta\varepsilon||$ for a single strain probe). More precisely, this means that the instantaneous modulus describing fabric change in terms of a strain increment can also depend on the direction α of the strain probe. Therefore, a condition of incremental linearity would invariably pose restrictions on the functions ψ_1 and ψ_2, as will be discussed later in Section 4.3.

3. DEM Simulations

Two-dimensional DEM simulations have been performed, using the PFC2D simulation code [12], on square assemblies of $50,000$ circular particles with uniformly distributed radii and a ratio of maximum to minimum particle radii of $r_{\max}/r_{\min} = 2$. The elastic part of the contact model is considered to be linear with stiffness constants, k_n and k_t, that are the same for both normal

and tangential directions, i.e. $k_n = k_t$. The normal stiffness k_n is selected such that $k_n/p_0 = 2 \times 10^2$, where p_0 is the initial confining pressure. The contact forces satisfy the Coulomb friction criterion $|f_t^c| \leq \mu f_n^c$, where f_n^c and f_t^c are the normal and tangential components of the force at contact c, respectively, with a friction coefficient of $\mu = 0.5$.

To prepare the various numerical samples, a relatively sparse cloud of particles was first generated. Then, the frictionless confining walls were moved toward each other until the required stress was attained. In this initial compaction stage, the friction coefficient was (artificially) reduced from its assumed value $\mu = 0.5$ in order to obtain granular systems with different initial coordination numbers Z_0 and void ratios e_0. Both average stress and strain tensors were determined at the boundaries of the numerical samples.

In order to remain consistent with the stress and strain measurements on the external boundaries, the fabric parameters were determined by considering all the contacts, including particle-wall contacts. Upon direct comparison, the contribution of particle-wall contacts to the fabric evolution trends has been found to be negligible for the square-shape samples and the number of particles used in this study.

Since the sample's response to the probing is very sensitive to the stability of static equilibrium, we ensured that the average out-of-balance force δf always remains much smaller than the average contact force. Here, the time step and the loading rate in the simulations have been selected such that the ratio between average out-of-balance force to the average contact force f satisfies $\delta f/f \leq 10^{-5}$.

Furthermore, preliminary simulations showed that, for looser samples, local instabilities can be triggered upon application of the strain probes. When interpreting the results, the fundamental assumption of linear response is not satisfied. The study of incremental behaviour of granular assemblies in the presence of such local instabilities requires different treatments that involve averaging over a number of micro-avalanches. To avoid such instabilities, before applying the probes, the samples were subjected here to a small deviatoric loading/unloading cycle that would trigger any potentially unstable micro-

Table 1: Coordination number Z_0, void ratio e_0, and percentage of rattlers after compaction, of the initial isotropic samples.

Z_0	4.53	4.21	4.10	3.87	3.76	3.68
e_0	0.157	0.173	0.179	0.196	0.204	0.211
Rattlers %	1.20	2.14	2.66	4.00	4.56	5.03

avalanches.

Six initial samples, with coordination numbers Z_0 and void ratios e_0 as listed in Table 1, were prepared in order to also investigate the influence of the initial coordination number. The contact structure has been ensured to be isotropic prior to applying strain probes, with an initial fabric anisotropy $|a_{c0}| \leq 10^{-4}$.

After preparing a stable sample, strain probes with a magnitude of $||\Delta\boldsymbol{\varepsilon}|| = \sqrt{\Delta\varepsilon_{yy}^2 + \Delta\varepsilon_{xx}^2} = 2 \times 10^{-4}$ were then applied. This strain probe magnitude has been selected, based on multiple attempts, such that: (1) it is sufficiently small for the stress and fabric response to remain linear, and (2) it is also sufficiently large that the numbers of lost and gained contacts are large enough to obtain good statistical data to determine the contributions defined in Eq. 4 to the change in the fabric tensor $\Delta\boldsymbol{F}$. The issue of the proper selection of the stress (or strain) probe magnitude is also discussed in [17], in the context of analyzing the strain response to stress probing in triaxial tests.

Throughout this study, the strain increment direction, α in Fig. 1, was varied within 15° increments, thus sweeping the entire 360° with 24 probes. The contact sets $\mathbb{C}^{\text{final}}$ at the end of each strain probe have been compared to the initial contact set $\mathbb{C}^{\text{init}}$ in order to determine the sets of lost, gained and persistent contacts (see Eq. 3), and their respective contributions to contact fabric change (see Eq. 4).

4. DEM Results

Results from DEM simulations investigating into the nature of stress and fabric responses obtained for various strain probings on both dense and loose samples are presented next. Contact mechanism contributions to fabric changes are systematically studied through an analytical procedure based on harmonic functions and a representation theorem that was introduced earlier in the paper. The fitted harmonic functions are, herein, compared with conditions pertaining to incremental linearity, with the final results indicating a significant dependency on the probe direction, and hence incremental nonlinearity.

4.1. General observations

Figure 2 shows stress and fabric responses to the imposed strain probes for the dense sample with initial coordination number of $Z_0 = 4.53$. The stress increments have been made dimensionless with respect to the normal contact stiffness k_n. Both stress and fabric responses for the individual probes show (sufficiently) linear trends in relation to the magnitude of the strain increment $||\Delta\varepsilon|| = 2 \times 10^{-4}$, which justifies the appropriateness of this strain range used for strain probing. The observed symmetry of the responses with respect to the direction $\alpha = 45^\circ$ is expected due to the isotropy of the sample. Positive values of fabric change (upper-right of Fig. 2-(c)) correspond to the prevalence of contact gains, which is associated with compression (lower-left part of the stress and strain responses in Fig. 2-(a) and (b)). It is clear that the fabric response is incrementally nonlinear with respect to the strain increment, $\Delta\boldsymbol{\varepsilon}$, as it strongly depends on the strain probe direction α.

Figure 3 shows the dimensionless stress response of samples with different initial coordination numbers Z_0 (with the same strain probe size). For clarity of presentation, only the final states of strain and stress increments are plotted here. It was shown previously [11, 17] that the presence of even very small plastic strains is reflected in the deviation of the stress response envelope from an ellipse that describes an incrementally linear stress response to the strain probes.

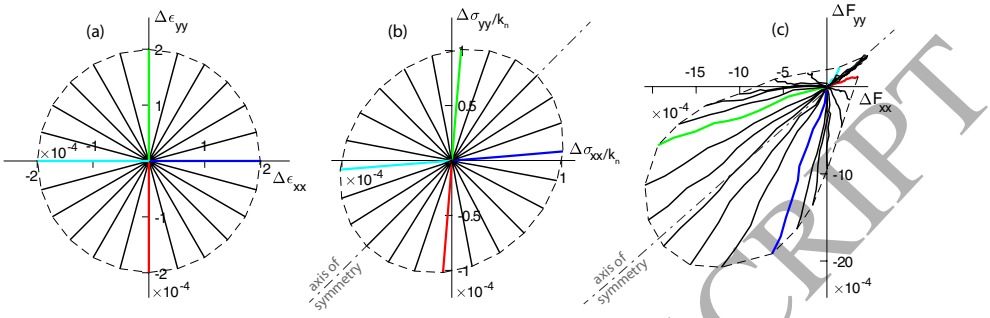

Figure 2: (a) Imposed strain probes, (b) stress responses, and (c) fabric responses. Results for the dense sample with initial coordination number $Z_0 = 4.53$. Some characteristic probe directions are shown in colour for easy interpretation and clarity.

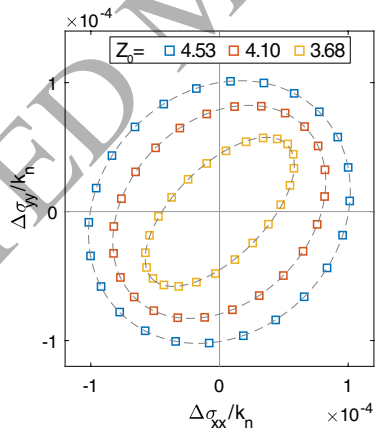

Figure 3: Dimensionless stress responses to the strain probes with magnitude of $||\Delta\varepsilon|| = 2 \times 10^{-4}$ for samples with different (selected) initial coordination numbers Z_0. Only the final points of the stress response have been plotted. The dashed lines represent elliptical fits that correspond to an incrementally linear stress response.

However, for the ranges of strains considered here in this study, the stress response is accurately described by an ellipse as plotted in dashed lines in Fig. 3. This indicates that the material response can be considered to be pseudo-elastic. A further numerical investigation to confirm this assertion involved simulating probes with an artificially large interparticle friction to suppress any sliding mechanism [42], which eventually showed insignificant plastic deformations. As a side note, the variation of the pseudo-elastic bulk and shear moduli with initial coordination number Z_0 (data not shown) is also consistent with previous numerical and analytical studies, see [25, 2, 42] for instance.

It is also of interest to examine the change in orientational distribution of the contributions of contact loss and gain mechanisms for characteristic probe directions, as shown in Fig. 4 for the fairly loose initial sample with $Z_0 = 3.68$, together with the second-order harmonic fit according to Eq. 5. While these results are not essential for the remainder of this study, Fig. 4 shows that the second-order harmonic functions describe the distributions sufficiently accurately when the numbers of lost or gained contacts are large enough for constructing a meaningful statistical distribution. For the cases considered in this study, the contributions of contact reorientation to the change of fabric are negligible, and hence have only been retained in the analyses to maintain generality.

It is also worth noticing that, despite the initially isotropic contact structure, the distributions of contact gain and loss exhibit slight directional dependency under isotropic compression and extension. However, these deviations are considered to be relatively insignificant as they have been shown to have negligible effect on the overall trends of fabric evolution with the probe direction.

While not presented here, the contact loss and gain distributions have been compared for pairs of supplementary probe angles which further confirmed the initial isotropy of the granular sample.

Overall, the results in Figure 4 show that, as expected, contact loss is more important than contact gain in probes that involve extension ($\alpha = 45°$, $\alpha = 90°$), while contact gain is more important than contact loss in probes that

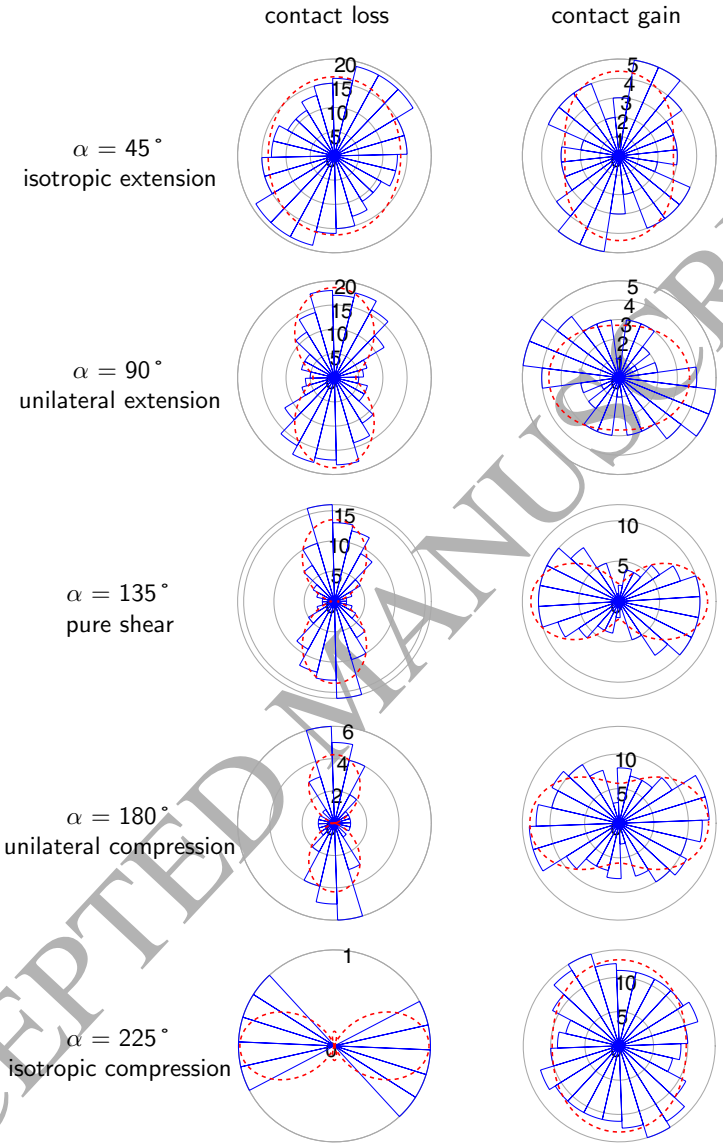

Figure 4: Change in orientational distribution of the number of contacts due to contact loss (left column), and contact gain (right column) for the sample with initial coordination number $Z_0 = 3.68$, subjected to different strain probe directions. The red dotted lines correspond to second-order harmonic fits. The numbers associated with the radius of the polar plots signify the number of lost or gained contacts in each directional bin.

involve compression ($\alpha = 180°$, $\alpha = 225°$). However, surprisingly, a fair number of contacts is still gained in isotropic extension ($\alpha = 45°$). In pure shear ($\alpha = 135°$), the numbers of lost and gained contacts are of the same order of magnitude. In isotropic compression and extension the orientational distributions can be considered to be isotropic (considering the limited statistical data). In unilateral extension ($\alpha = 90°$) contacts are mainly lost in the direction of extension, while a smaller number of contacts is gained in the direction perpendicular to the direction of extension. Similar, but opposite trends are observed for unilateral compression ($\alpha = 180°$).

The evolution of fabric is next investigated in terms of contact loss, gain, and reorientation tensors, $\Delta \boldsymbol{F}^l$, $\Delta \boldsymbol{F}^g$, and $\Delta \boldsymbol{F}^r$, as defined in Eq. 3. The principal directions of these tensors are aligned with the horizontal and vertical directions, as follows from Fig. 4. Therefore, the properties of these tensors are described here in terms of the sum of, and difference between their vertical and horizontal components (which are principal values). For generality, these values are normalized to the strain probe magnitude $||\Delta\boldsymbol{\varepsilon}||$ to indicate the rate of change with respect to strain increment:

$$\begin{aligned} \Delta Z^{*m} &= \frac{\Delta F^m_{yy} + \Delta F^m_{xx}}{||\Delta\boldsymbol{\varepsilon}||} = \Delta F^{*m}_{yy} + \Delta F^{*m}_{xx} \\ \Delta A^{*m} &= \frac{\Delta F^m_{yy} - \Delta F^m_{xx}}{||\Delta\boldsymbol{\varepsilon}||} = \Delta F^{*m}_{yy} - \Delta F^{*m}_{xx} \\ m &= l,\ g,\ r \quad \text{for contact loss, gain, and reorientation} \end{aligned} \tag{10}$$

Recalling the definition in Eq. 2, the parameter ΔZ^{*m} in Eq. 10 denotes the rate of change in coordination number due to each mechanism, while ΔA^{*m} is related to the associated rate of change of fabric anisotropy. However, unlike the anisotropy measure in Eq. 2, the variable ΔA^{*m} in Eq. 10 is defined such that, depending on the direction of the maximum fabric change, it can assume both positive and negative values. The variation of ΔZ^{*m} and ΔA^{*m} with probe direction α is shown in Fig. 5 for the probes presented in Fig. 3.

The symmetry around $\alpha = 45°$, as expected for initially isotropic samples, is observed for all initial coordination numbers Z_0. The maximum change in

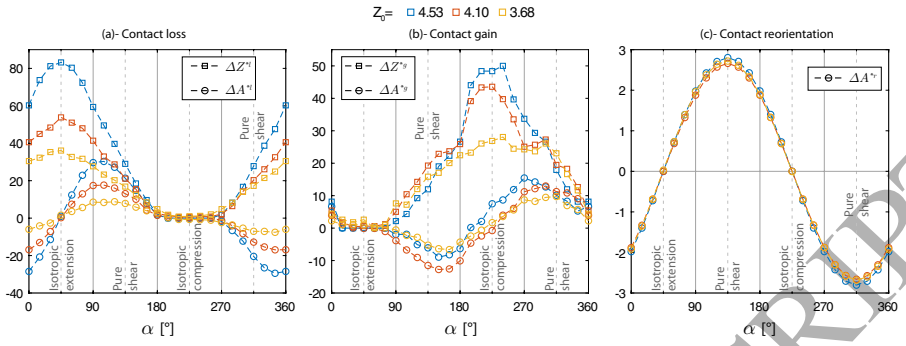

Figure 5: Rate of change in contact fabric tensor due to (a) contact loss, (b) contact gain, and (c) contact reorientation, as defined in Eq. 3 for strain probes shown in Fig. 3. The square symbols show the sum of the vertical and horizontal (principal) components of the tensors, and the circles show the difference between these two values, as defined in Eq. 10. The contribution of contact reorientation to coordination number, ΔZ^{*r} is not presented as it is always zero by definition, see Eqs. 3 and 4.

coordination number due to contact loss and contact gain is obtained for $\alpha = 45°$ (isotropic extension) and $\alpha = 225°$ (isotropic compression), respectively. However, the rate of contact loss in isotropic extension is not the same as the rate of contact gain in isotropic compression, which leads to the asymmetry of fabric change around $\alpha = 135°$, as observed earlier in Fig.2-(c). The value of ΔZ^{*r} (not presented in Fig. 5) is always zero because, by definition, the number of contacts does not change due to contact reorientation, see Eqs. 3 and 4. The rate of change in fabric due to contact reorientation is much smaller than that due to contact loss and gain. As expected, the rates of change in the fabric tensor (ΔZ^{*m} and ΔA^{*m}) increase with initial coordination number Z_0, both for loss and gain ($m = l, g$). However, no clear dependency on initial coordination number is observed for the contribution from contact reorientation in Fig. 5-(c).

The results shown in Figs. 5-(a) and (b) show that the maximum change in fabric anisotropy parameter, ΔA^{*m}, does not occur for the directions of pure shear, $\alpha = 135°$ and $315°$. The directions of these extrema are shifted slightly towards the extension half region of the probes, i.e. $-45° < \alpha < 135°$.

This indicates that the largest change in fabric anisotropy occurs for a strain probe direction that involves a combination of deviatoric and extension strain. Note that such deviations from pure shear directions are consistent with the expression in Eq. 8, as is demonstrated later.

It is also worth noticing in Figs. 5-(a) and (b) that, regardless of initial coordination number, zones exist around directions of isotropic extension at $\alpha = 45°$ (or isotropic compression at $\alpha = 225°$) where contact gains (or contact losses) remain negligible. The existence of such zones has been previously predicted by [41] where the orientational distribution of contact gains and losses has been determined, based on the orientational change in average contact force. The complementary analysis provided in Appendix A shows that these zones correspond to $18.5° < \alpha < 63.5°$ for zero contact gain, and $198.5° < \alpha < 251.5°$ for zero contact loss, which are confirmed with good accuracy by the results in Fig. 5.

4.2. Analysis of DEM results with Representation Theorem

Recalling the representation theorem for the functional dependence of a second-order tensor on another second-order tensor in two-dimensional isotropic systems, as introduced in Eq. 8, it follows that the change in fabric due to each mechanism can be conveniently expressed as:

$$\Delta F_{ij}^{*m} = \psi_1^m \delta_{ij} + \psi_2^m \Delta\varepsilon_{ij}^*, \quad m = l,\ g,\ r \tag{11}$$

with ψ_1^m and ψ_2^m being functions of the invariants of $\Delta\boldsymbol{\varepsilon}^*$ given in Eq. 9 and of the initial coordination number, Z_0, while

$$\psi_1 = \psi_1^g - \psi_1^l + \psi_1^r, \quad \psi_2 = \psi_2^g - \psi_2^l + \psi_2^r \tag{12}$$

intrinsically account for the contribution of each individual mechanism as per Eq. 4.

The variables ΔZ^{*m} and ΔA^{*m}, defined in Eq. 10, can now also be expressed

in terms of ψ_1^m and ψ_2^m, i.e.

$$\begin{aligned}\Delta Z^{*m} &= \Delta F_{yy}^{*m} + \Delta F_{xx}^{*m} = 2\psi_1^m + \psi_2^m(\cos\alpha + \sin\alpha)\\ \Delta A^{*m} &= \Delta F_{yy}^{*m} - \Delta F_{xx}^{*m} = \psi_2^m(\cos\alpha - \sin\alpha)\\ m &= l,\ g,\ r\end{aligned} \tag{13}$$

Furthermore, an assessment of the results in Fig. 5 has shown that the variation of fabric changes with strain probe direction α can be well represented by truncated, second-order harmonic series. By combining this observation with the expressions in Eq. 13 and noting that ψ_1 and ψ_2 are functions of the invariants defined in Eq. 9, we obtain that ψ_1^m and ψ_2^m should depend linearly on the invariants as follows:

$$\begin{aligned}\psi_1^m &= B^m + C^m(\cos\alpha + \sin\alpha) + D^m\cos\alpha\,\sin\alpha\\ \psi_2^m &= E^m + G^m(\cos\alpha + \sin\alpha)\\ m &= g,\ l,\ r\end{aligned} \tag{14}$$

with B^m, C^m, D^m, E^m, and G^m being the five coefficients describing the variation of fabric change with respect to strain probe direction α for each mechanism. These coefficients are independent of α and only depend on the initial coordination number Z_0 of the granular sample. Substitution of Eq. 14 into Eq. 13 gives:

$$\begin{aligned}\Delta Z^{*m} =& (2B^m + G^m) + (2C^m + E^m)(\cos\alpha + \sin\alpha)\\ &+2(D^m + G^m)\cos\alpha\,\sin\alpha\\ \Delta A^{*m} =& E^m(\cos\alpha - \sin\alpha) + G^m(\cos^2\alpha - \sin^2\alpha)\\ &m = g,\ l,\ r\end{aligned} \tag{15}$$

Only a single coefficient, E^r, is required to represent the variation of fabric tensor due contact reorientation ΔF_{ij}^r, since no coordination number change is associated with contact reorientation, and the variation of ΔA^{*r} is accurately fitted with the first-order harmonic term, as demonstrated in Fig.6-(c).

Figure 6 shows the accuracy of the expressions in Eq. 15 towards matching the variation of ΔZ^{*m} and ΔA^{*m} from DEM simulations, with strain probe

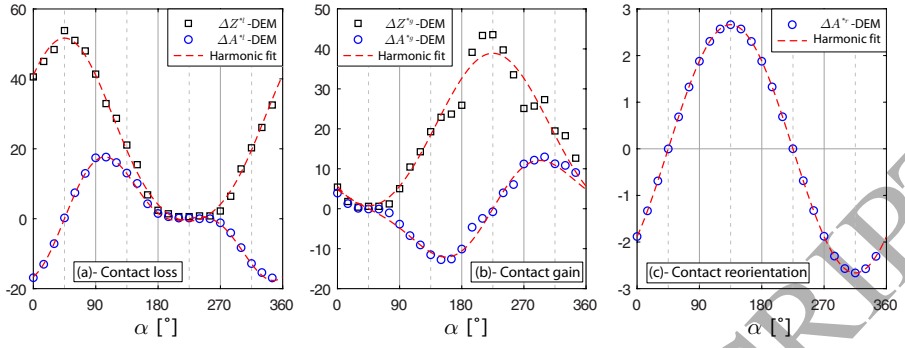

Figure 6: Accuracy of the expressions in Eq. 15 in representing fabric change due to contact loss (left), contact gain (middle), and contact reorientation (right), for the sample with initial coordination number $Z_0 = 4.10$.

direction α for the sample with initial coordination number of $Z_0 = 4.10$, where a good to an acceptable consistency between the DEM results and the fitted curves is obtained.

For a more physically meaningful representation, the coefficients describing the variation of ΔZ^{*m} are replaced with the values of ΔZ^{*m} at the characteristic probe orientations $\alpha = 45°$ (isotropic extension), $\alpha = 135°$ (pure shear), and $\alpha = 225°$ (isotropic compression). The relation between ΔZ^{*m} in these characteristic probe directions, and the coefficients in Eq. 15 is given by:

$$\begin{aligned} \Delta Z^{*m}|_{\alpha=45°} &= 2B^m + 2G^m + \sqrt{2}(2C^m + E^m) + D^m \\ \Delta Z^{*m}|_{\alpha=225°} &= 2B^m + 2G^m - \sqrt{2}(2C^m + E^m) + D^m \\ \Delta Z^{*m}|_{\alpha=135°} &= 2B^m - D^m \end{aligned} \tag{16}$$

The variation of ΔA^{*m} is (still) expressed in terms of the coefficients E^m and G^m.

The effect of initial coordination number Z_0 on the fabric evolution can now be represented by the variation of the coefficients in Eq. 16 with Z_0 for contact loss and gain mechanisms, as shown in Fig. 7. More samples (total of six; see Table 1) with different initial conditions have been studied here for better visualization of the trends. The single characteristic value associated with contact reorientation remains relatively constant at $E^r \sim 2.7$ for the range

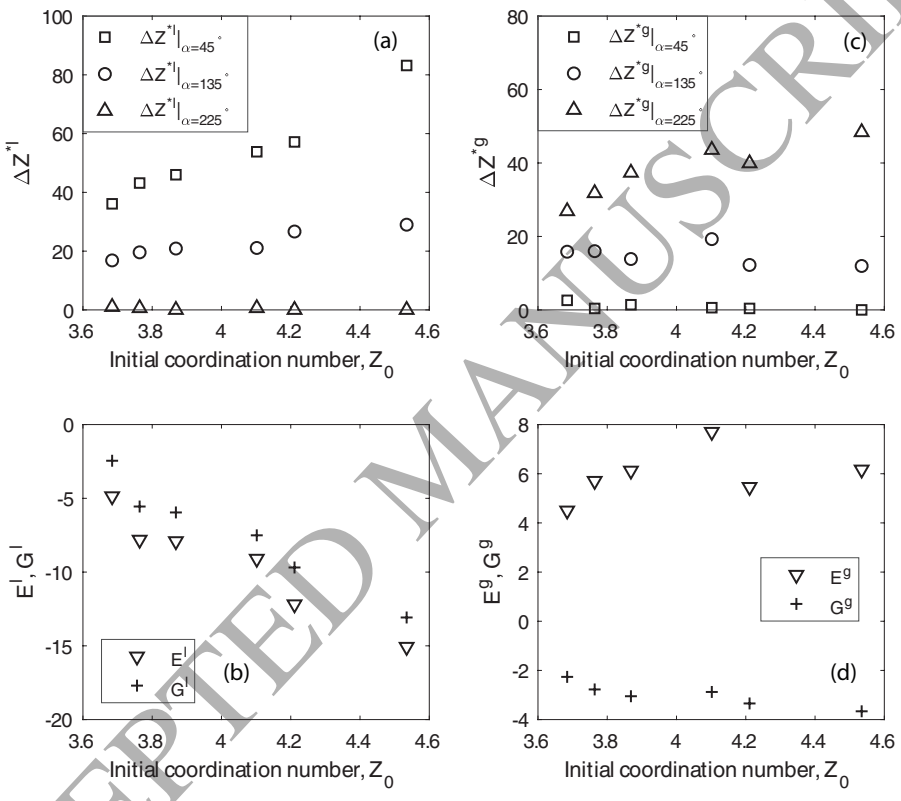

Figure 7: Variation of coefficients in Eq. 15 and 16 with initial coordination number Z_0 for contact loss (a and b), and contact gain (c and d).

of initial coordination numbers, Z_0, studied here.

A general trend can be observed in Figs. 7-(a) and (b) for contact gain and loss, where the magnitude of all characteristic values increases with initial coordination number Z_0. Such a monotonic increase of the coefficients suggests a scaling of fabric changes with initial number of contacts, as expected. Moreover, the values for contact loss and gain along isotropic compression and extension respectively, i.e. $\Delta Z^{*l}|_{\alpha=225^\circ}$ and $\Delta Z^{*g}|_{\alpha=45^\circ}$, are expectedly negligible. On the other hand, the difference between contact loss in isotropic extension, $\Delta Z^{*l}|_{\alpha=45^\circ}$, and contact gain in isotropic compression, $\Delta Z^{*g}|_{\alpha=225^\circ}$, already points to the origin of the incremental nonlinearity of the fabric evolution with strain. For pure shear directions, both contact loss and gain rates are weakly dependent on the initial coordination number Z_0 of the sample.

4.3. Conditions for incremental linearity of fabric response

The origin of the incremental nonlinearity of the fabric response is further investigated by formulating conditions under which a linear response is obtained. Analogous to the stress-strain relationship for isotropic, linear elasticity [8], the general expression for incrementally linear behaviour of isotropic materials is:

$$\Delta F_{ij}^{*m} = \lambda_1^m \mathrm{tr}(\Delta\boldsymbol{\varepsilon}^{\boldsymbol{*}})\delta_{ij} + \lambda_2^m \Delta\varepsilon_{ij}^{*} \tag{17}$$

where λ_1^m and λ_2^m are coefficients that are independent of the loading direction.

A comparison of Eqs. 11 and 17 gives $\psi_1^m = \lambda_1^m \mathrm{tr}(\Delta\boldsymbol{\varepsilon}^{\boldsymbol{*}})$ and $\psi_2^m = \lambda_2^m$. By combining these expressions with Eqs. 9, 12 and 14, conditions are obtained for the *total* fabric change to be incrementally linear:

$$\begin{aligned} B^g - B^l &= 0 \\ D^g - D^l &= 0 \\ G^g - G^l + G^r &= 0 \end{aligned} \tag{18}$$

Note that $B^r = 0$ and $D^r = 0$, as no change in coordination number occurs due to contact reorientation, $\Delta Z^{*r} = 0$.

The first two relations in Eq. 18 imply, using Eq. 15, that $\Delta Z^*|_{\alpha=45^\circ} = -\Delta Z^*|_{\alpha=225^\circ}$. Moreover, Figs. 7(a) and (c) show that the rate of contact loss in isotropic compression, $\Delta Z^{*l}|_{\alpha=225^\circ}$, and that of contact gain in isotropic extension, $\Delta Z^{*g}|_{\alpha=45^\circ}$, are very small. Hence it follows that $\Delta Z^{*l}|_{\alpha=45^\circ} = \Delta Z^{*g}|_{\alpha=225^\circ}$. Thus, the first condition for incremental linearity is that the rate of change in coordination number due to contact loss in isotropic extension must be equal to the rate of change in coordination number due to contact gain in isotropic compression.

From Eqs. 14 and 18 it follows that $\Delta Z^*|_{\alpha=135^\circ} = 0$, and hence $\Delta Z^{*l}|_{\alpha=135^\circ} = \Delta Z^{*g}|_{\alpha=135^\circ}$. Thus, the second condition for incremental linearity is that in pure shear the rates of change in coordination number due to contact loss and contact gain must be equal.

Finally, from Eqs. 15 and 18, it follows that $\max(\Delta A^*) = \Delta A^*|_{\alpha=135^\circ}$, and as such, the third condition for incremental linearity is that the maximum rate of change of anisotropy is obtained in pure shear.

In summary, an incrementally linear fabric response is obtained whenever all the following conditions are met:

1. The rate of change in coordination number due to contact loss in isotropic extension is equal to the rate of change in coordination number due to contact gain in isotropic compression.
2. The rates of change in coordination number due to contact loss and contact gain are equal in pure shear.
3. The maximum rate of change of contact anisotropy is obtained in pure shear.

4.4. Incrementally nonlinear character of fabric changes

Interpreting the numerical results within the framework developed in the previous subsection, we see that none of the above three conditions is satisfied, as demonstrated by the results depicted in Fig. 5, where the deviation from the first condition is the largest.

A more quantitative assessment of the incremental nonlinearity of fabric evolution can be obtained by investigating the variables ΔZ^* and ΔA^* associated with the total fabric change, which, following Eq. 4, can now be expressed as:

$$\begin{aligned}
\Delta Z^* &= -\Delta Z^{*l} + \Delta Z^{*g} = a_1 + a_2(\cos\alpha + \sin\alpha) + a_3 \cos\alpha \sin\alpha \\
\Delta A^* &= -\Delta A^{*l} + \Delta A^{*g} + \Delta A^{*r} = a_4(\cos\alpha - \sin\alpha) + a_5(\cos^2\alpha - \sin^2\alpha) \\
a_1 &= -(2B^l + G^l) + (2B^g + G^g) \\
a_2 &= -(2C^l + E^l) + (2C^g + E^g) \\
a_3 &= -2(D^l + G^l) + 2(D^g + G^g) \\
a_4 &= -E^l + E^g + E^r \\
a_5 &= -G^l + G^g
\end{aligned} \tag{19}$$

Conditions in Eq. 18 require the coefficients a_1, a_2, and a_3 to be equal to zero for the variations in Eq. 19 to be incrementally linear.

The variation of coefficients in Eq. 19 with initial coordination number is given in Fig. 8, where non-zero values of variables a_1, a_3, and a_5 point towards an incrementally nonlinear evolution of fabric with strain increments. Based on the expressions in Eq. 19, the fact that $a_5 < a_3$ indicates that the deviation from incremental linearity is more significant in the deviatoric part of fabric tensor (characterized by ΔA^*) compared to its spherical part (characterized by ΔZ^*). As also mentioned in relation to Fig. 7, the changes in fabric appear to scale with initial coordination number as suggested by the almost linear trends in Fig. 8.

The studies in [1, 3] conclusively demonstrate that, depending on the sample preparation method, the initial coordination number and void ratio of the granular sample can vary almost independently, and as such, a comprehensive parametric study should ideally consider the effect of these variables separately. While such an extensive investigation is beyond the scope of the current study, one can expect, based on arguments in [41] that the contact loss mechanism depends mainly on coordination number, and the contact gain mechanism on the

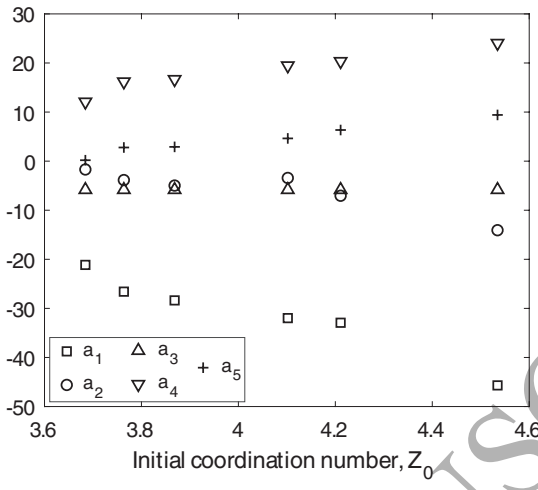

Figure 8: Variation of coefficients describing the total fabric change in Eq. 19 with initial coordination number Z_0.

void ratio. The latter dependency originates from the fact that for new contacts to form, the neighbouring particles need to close their interparticle gap, which is a function of void ratio.

To recapitulate findings, the results for normalized total fabric change, as well as the contributions of contact gain and loss to the fabric change, for the strain probes shown in Fig. 5 can be compiled together with the strain probes and stress responses in Fig. 3, to illustrate the correlations between the changes in contact fabric, and isotropic and deviatoric components of stress and strain increments, as shown in Fig. 9. The isotropic (or spherical) and deviatoric components stress and strain are defined as:

$$\begin{aligned} \Delta p = \frac{1}{2}(\Delta\sigma_{yy} + \Delta\sigma_{xx}), \quad \Delta q = \frac{1}{2}(\Delta\sigma_{yy} - \Delta\sigma_{xx}) \\ \Delta\varepsilon_v = \Delta\varepsilon_{yy} + \Delta\varepsilon_{xx}, \quad \Delta\varepsilon_s = \Delta\varepsilon_{yy} - \Delta\varepsilon_{xx} \end{aligned} \tag{20}$$

As expected, the spherical part of fabric changes due to contact loss and gain, ΔZ^{*l}, ΔZ^{*g} show relatively monotonic trends with spherical stress and strains. Such a linearity is even more clear for the spherical component of the total fabric change, ΔZ^*, which suggests that the relation between ΔZ^*

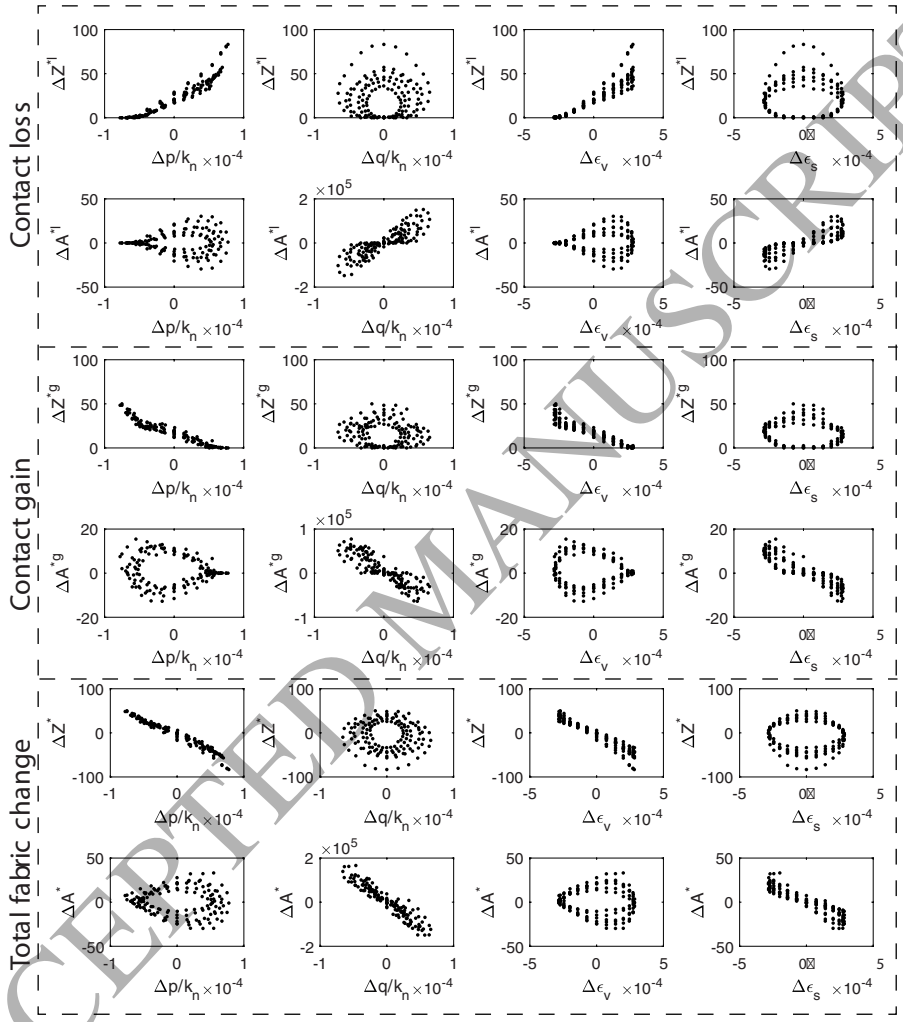

Figure 9: Correlation between the fabric changes due to contact loss and gain, and total fabric change, and the volumetric and deviatoric components of stress and strain increments. Stress increments are presented in dimensionless form.

and the hydrostatic stress and volumetric pressure is independent of the probe direction. Moreover, the linearity in the case of the spherical component of the fabric change is more evident in terms of stress increments. On the other hand, the deviatoric fabric terms, ΔA^{*l}, ΔA^{*g}, and ΔA^{*}, show more scattered variations and less robust correlations with the stress and strain terms, which indicates that the relation between contact fabric and strain (or stress) changes depends on probe direction, and hence, is incrementally nonlinear in nature. Such a dependency on the direction of loading further advocates the directional dependency of plastic flow rule [51] and constitutive models embedding such incremental nonlinearity [13, 14, 34].

It is also of interest to study a wider range of contact stiffness to verify the generality of the conclusions. For this case, our preliminary results show that the general trends of fabric evolution with strain probe direction remain the same when contact stiffness is varied.

5. Conclusions

The stress and fabric responses of granular media to strain probing have been studied, based on two-dimensional DEM simulations of initially isotropic systems with various coordination numbers and void ratios. Within sufficiently high numerical accuracy, the strain probe size was selected small enough to obtain a linear stress response, but large enough to cause sizeable fabric changes that are reliable for determining their dependency on the strain probe direction.

Intriguingly, the DEM simulation results show that while the stress response is incrementally linear and pseudo-elastic, the associated fabric changes are instead dependent on the strain probe direction, and hence incrementally nonlinear. This incremental nonlinearity of the fabric response appears already in the small deformation regime and can only develop further to serve as a precursor to the elasto-plasticity of anisotropic granular assemblies. It also raises the issue of how fabric, as an internal state variable, is related to deformations and stresses in a granular medium. The stress-strain response of the samples re-

mained incrementally linear despite of the strong directional dependency of the fabric evolution. As such, this indicates that the initial pseudo-elastic response is unaffected by the change in contact fabric, at least for the isotropic assemblies and the stiffness range considered in this study. However, this conclusion does not extend straightforwardly to stiffer and/or anisotropic assemblies where subtle effects of fabric change on pseudo-elastic response can be envisaged [41].

To further explore the nature of fabric changes, the contributions of each of the following three mechanisms, i.e. contact loss, contact gain and contact reorientation, have been separately quantified for each strain probe direction. The contribution due to contact reorientation is found to be small in comparison to contributions due to contact loss and contact gain. By contrast, contact loss is dominant over contact gain in probes that involve extensional strains, while the opposite is observed in compressive strain probes.

A detailed analysis of the evolution of fabric changes has been conducted using second-order tensors to describe distributions for changes in contact orientations, including the three mechanisms for all probing directions. As such, combining a representation theorem for isotropic tensorial functions with the results of the DEM simulations yields expressions that relate changes in coordination number and anisotropy for each strain probe direction with a relatively small number of parameters that only depend on the initial coordination number of the sample. These parameters have been expressed in terms of the rate of change of coordination number for certain characteristic directions: isotropic compression, isotropic extension and pure shear.

Additionally, as main findings of this work, the following special cases related to the nature of fabric changes have been distinguished:

1. In isotropic compression the rate of change in coordination number due to contact loss is very small, while for the isotropic extension the rate of contact gain is very small.
2. The rate of change in anisotropy is not largest in pure shear, but in a probe direction that involves shear *and* extension.

3. The rate of contact loss in isotropic extension is larger than the rate of contact gain in isotropic compression. It is this difference that ultimately forms the primary origin of the incremental nonlinearity of fabric response to strain probing.
4. The parameters expressing the rate of change in the above-mentioned characteristic directions scale almost linearly with initial coordination number of the samples.

The issue of 'microstructure-motivated' elasticity remains an open question that requires further studies, with wider ranges of conditions to clearly understand and explain the evolution of contact fabric and its role in driving the mechanical response of granular materials, especially in three-dimensional conditions. In particular, it will be interesting to study the fabric evolution in initially anisotropic configurations, for which, as our preliminary results show, interrelations have been observed between lost and and gained contacts distributions. These interrelations should also be studied from a static equilibrium point of view for loose samples where the coordination number must also satisfy the minimum jamming transition threshold. By including simulations with wider ranges of contact stiffness values, and particularly stiffer contacts, samples can be prepared with initial coordination numbers closer to the isostaticity limit, where, according to previous studies, distinct behaviours in terms of dilatancy and fabric evolution are expected [37, 38, 4].

6. Acknowledgements

Research funding jointly provided by the Natural Sciences and Engineering Research Council of Canada and Foundation Computer Modelling Group (now Energi Solutions Ltd) is gratefully acknowledged. This work was initiated during a short research visit at the University of Twente, the Netherlands, by the first author. Sincere gratitude is due to the University of Twente for providing an enriching and stimulating environment for this work, which has subsequently flourished into this manuscript.

References

References

[1] Agnolin, I. and J.-N. Roux (2007a). Internal states of model isotropic granular packings. i. assembling process, geometry, and contact networks. *Physical Review E 76*(6), 061302.

[2] Agnolin, I. and J. N. Roux (2007b). Internal states of model isotropic granular packings. III. Elastic properties. *Physical Review E - Statistical, Nonlinear, and Soft Matter Physics 76*(6), 061304.

[3] Agnolin, I. and J.-N. Roux (2008). On the elastic moduli of three-dimensional assemblies of spheres: Characterization and modeling of fluctuations in the particle displacement and rotation. *International Journal of Solids and Structures 45*(3-4), 1101–1123.

[4] Azéma, É., F. Radjaï, and J.-N. Roux (2015). Internal friction and absence of dilatancy of packings of frictionless polygons. *Physical Review E 91*(1), 010202.

[5] Azéma, E., F. Radjai, and G. Saussine (2009). Quasistatic rheology, force transmission and fabric properties of a packing of irregular polyhedral particles. *Mechanics of Materials 41*(6), 729–741.

[6] Bagi, K. (1996). Stress and strain in granular assemblies. *Mechanics of Materials 22*(3), 165–177.

[7] Bagi, K. (2006). Analysis of microstructural strain tensors for granular assemblies. *International Journal of Solids and Structures 43*(10), 3166–3184.

[8] Bardet, J. (1994). Numerical simulations of the incremental responses of idealized granular materials. *International Journal of Plasticity 10*(8), 879–908.

[9] Bashir, Y. and J. Goddard (1991). A novel simulation method for the quasi-static mechanics of granular assemblages. *Journal of Rheology 35*(5), 849–885.

[10] Calvetti, F., G. Combe, and J. Lanier (1997). Experimental micromechanical analysis of a 2d granular material: relation between structure evolution and loading path. *Mechanics of Cohesive-frictional Materials 2*(2), 121–163.

[11] Calvetti, F., G. Viggiani, and C. Tamagnini (2003). A numerical investigation of the incremental behavior of granular soils. *Rivista Italiana di Geotecnica 37*(3), 11–29.

[12] Cundall, P. and O. Strack (1999). Particle flow code in 2 dimensions. *Itasca consulting group, Inc.*

[13] Darve, F. (1990). The expression of rheological laws in incremental form and the main classes of constitutive equations. *Geomaterials: Constitutive Equations and Modelling*, 123–148.

[14] Darve, F. and F. Nicot (2005). On incremental non-linearity in granular media: phenomenological and multi-scale views (part i). *International journal for numerical and analytical methods in geomechanics 29*(14), 1387–1409.

[15] Del Piero, G. (1998). Representation theorems for hemitropic and transversely isotropic tensor functions. *Journal of Elasticity 51*(1), 43–71.

[16] Drescher, A. and G. de Josselin de Jong (1972). Photoelastic verification of a mechanical model for the flow of a granular material. *Journal of the Mechanics and Physics of Solids 20*(5), 337–340.

[17] Froiio, F. and J. N. Roux (2010). Incremental response of a model granular material by stress probing with dem simulations. In *IUTAM-ISIMM Symposium on mathematical modeling and physical instances of granular flow, Sep 2009, Reggio Calabria, Italy, AIP Conference Proceedings, eds. J. D. Goddard, J. T. Jenkins, P. Giovine*, Volume 1227, pp. 183–197. American Institute of Physics.

[18] Gao, Z. and J. Zhao (2017). A non-coaxial critical-state model for sand accounting for fabric anisotropy and fabric evolution. *International Journal of Solids and Structures 106–107*, 200–212.

[19] Gudehus, G. (1979). A comparison of some constitutive laws for soils under radially symmetric loading and unloading. *Canadian Geotechnical Journal 20*, 502–516.

[20] Guo, N. and J. Zhao (2013). The signature of shear-induced anisotropy in granular media. *Computers and Geotechnics 47*, 1–15.

[21] Horne, M. (1965). The behaviour of an assembly of rotund, rigid, cohesionless particles. i and ii. *Proceedings of the Royal Society of London A 286*(1404), 62–97.

[22] Kanatani, K. I. (1984). Distribution of directional data and fabric tensors. *International Journal of Engineering Science 22*(2), 149–164.

[23] Kruyt, N. P. (2012). Micromechanical study of fabric evolution in quasi-static deformation of granular materials. *Mechanics of Materials 44*, 120–129.

[24] Kruyt, N. P. and L. Rothenburg (1996). Micromechanical definition of the strain tensor for granular materials. *J. Appl. Mech. 118*, 706–711.

[25] Kruyt, N. P. and L. Rothenburg (1998). Statistical theories for the elastic moduli of two-dimensional assemblies of granular materials. *International Journal of Engineering Science 36*(10), 1127–1142.

[26] Kruyt, N. P. and L. Rothenburg (2006). Shear strength, dilatancy, energy and dissipation in quasi-static deformation of granular materials. *Journal of Statistical Mechanics: Theory and Experiment 2006*(07), P07021.

[27] Kruyt, N. P. and L. Rothenburg (2014). On micromechanical characteristics of the critical state of two-dimensional granular materials. *Acta Mechanica 225*, 2301–2318.

[28] Kruyt, N. P. and L. Rothenburg (2016). A micromechanical study of dilatancy of granular materials. *Journal of the Mechanics and Physics of Solids 95*, 411–427.

[29] Kuhn, M. R. (1999). Structured deformation in granular materials. *Mechanics of materials 31*(6), 407–429.

[30] Li, X. and X.-S. Li (2009). Micro-macro quantification of the internal structure of granular materials. *Journal of engineering mechanics 135*(7), 641–656.

[31] Li, X. S. and Y. F. Dafalias (2002). Constitutive modeling of inherently anisotropic sand behavior. *Journal of Geotechnical and Geoenvironmental Engineering 128*(10), 868–880.

[32] Li, X. S. and Y. F. Dafalias (2011). Anisotropic critical state theory: role of fabric. *Journal of Engineering Mechanics 138*(3), 263–275.

[33] Love, A. E. H. (1927). *A Treatise on the Mathematical Theory of Elasticity*. Cambridge University Press.

[34] Nicot, F. and F. Darve (2007). Basic features of plastic strains: from micro-mechanics to incrementally nonlinear models. *International Journal of Plasticity 23*(9), 1555–1588.

[35] Oda, M. (1972). Initial fabrics and their relations to mechanical properties of granular material. *Soils and foundations 12*(1), 17–36.

[36] Oda, M., S. Nemat-Nasser, and M. M. Mehrabadi (1982). A statistical study of fabric in a random assembly of spherical granules. *International Journal for Numerical and Analytical Methods in Geomechanics 6*(1), 77–94.

[37] Peyneau, P.-E. and J.-N. Roux (2008a). Frictionless bead packs have macroscopic friction, but no dilatancy. *Physical review E 78*(1), 011307.

[38] Peyneau, P.-E. and J.-N. Roux (2008b). Solidlike behavior and anisotropy in rigid frictionless bead assemblies. *Physical Review E 78*(4), 041307.

[39] Pouragha, M. and R. Wan (2016a). Onset of Structural Evolution in Granular Materials as a Redundancy Problem. *Granular Matter 18*.

[40] Pouragha, M. and R. Wan (2016b). Strain in granular media – a probabilistic approach to Dirichlet tessellation. *Journal of Engineering Mechanics*, C4016002.

[41] Pouragha, M. and R. Wan (2017). Non-dissipative structural evolutions in granular materials within the small strain range. *International Journal of Solids and Structures 110*, 94–105.

[42] Pouragha, M. and R. Wan (2018). On elastic deformations and decomposition of strain in granular media. *International Journal of Solids and Structures*.

[43] Pouragha, M., R. Wan, and N. Hadda (2014). A microstructural plastic potential for granular materials. *Geomechanics from micro to macro*, 661–665.

[44] Radjai, F., H. Troadec, and S. Roux (2004). Key features of granular plasticity. In *Granular materials: fundamentals and applications*, pp. 157–184. Royal Society of Chemistry London.

[45] Rothenburg, L. and R. Bathurst (1989). Analytical study of induced anisotropy in idealized granular materials. *Géotechnique 39*(4), 601–614.

[46] Rothenburg, L. and N. P. Kruyt (2004). Critical state and evolution of coordination number in simulated granular materials. *International Journal of Solids and Structures 41*(21), 5763–5774.

[47] Rothenburg, L. and A. Selvadurai (1981). A micromechanical definition of the cauchy stress tensor for particulate media. *Mechanics of Structured Media*, 469–486.

[48] Satake, M. (1978). Constitution of mechanics of granular materials through the graph theory. In *Proc. US-Japan Seminar on Continuum Mech. Stat. Appr. Mech. Granul. Mater., Sendai*, pp. 203–215.

[49] Thornton, C. and L. Zhang (2010). On the evolution of stress and microstructure during general 3d deviatoric straining of granular media. *Géotechnique 60*(5), 333–341.

[50] Tobita, Y. (1989). Fabric tensors in constitutive equations for granular materials. *Soils and Foundations 29*(4), 91–104.

[51] Wan, R. and M. Pinheiro (2014). On the validity of the flow rule postulate for geomaterials. *International Journal for Numerical and Analytical Methods in Geomechanics 38*(8), 863–880.

[52] Wan, R. and M. Pouragha (2014). Fabric and connectivity as field descriptors for deformations in granular media. *Continuum Mechanics and Thermodynamics 27*(1-2), 243–259.

[53] Wan, R. G. and J. Guo (2001). Drained cyclic behavior of sand with fabric dependence. *Journal of Engineering Mechanics 127*(11), 1106–1116.

[54] Weber, J. (1966). Recherches concernant les contraintes intergranulaires dans les milieux pulvérulents. *Bul. liaison P. et Ch 2*(64), 170.

[55] Zhu, H., M. M. Mehrabadi, and M. Massoudi (2006). Three-dimensional constitutive relations for granular materials based on the dilatant double shearing mechanism and the concept of fabric. *International journal of plasticity 22*(5), 826–857.

Appendix A. Zones with Zero Contact Gain and Loss

Following the analysis in [41], probing zones can be identified that are associated with zero contact gain and loss. Equation 18 in [41] gives the change in average contact force along direction θ as:

$$d\bar{f_n}^*(\theta) = \langle f_n \rangle \frac{dp}{p} \left[1 + \cos 2\theta \left(a_n + 2\frac{dq}{dp} - 2\frac{q}{p} \right) \right] \tag{A.1}$$

where a_n is the anisotropy of the normal contact forces, $\langle f_n \rangle$ is the average normal contact force, and θ is the direction in space. Moreover, as a simplifying

assumption, and based on the results in Fig. 2, the direction of stress response is assumed to be the same as the strain probe direction α. In this case the incremental stress ratio, dq/dp can be written as:

$$\frac{dq}{dp} = \frac{\sin\alpha - \cos\alpha}{\sin\alpha + \cos\alpha} \tag{A.2}$$

By substituting Eq. A.2 into A.1, and assuming that $a_n = 0$ and $q = 0$ for initially isotropic cases considered in the current study, the directional change in average contact force can be related to probe direction:

$$d\bar{f_n}^*(\theta) = \langle f_n \rangle \frac{dp}{p} \left[1 + \cos 2\theta \left(2\,\frac{\sin\alpha - \cos\alpha}{\sin\alpha + \cos\alpha}\right)\right] \tag{A.3}$$

Based on the arguments offered in [41], contacts are lost along directions θ where $d\bar{f_n}^*(\theta)$ is negative and gained where it is positive. However, it can be shown that for specific ranges of probe direction, α, the change in average contact force remains positive (or negative) for all values of θ. These ranges can be determined by first finding the minimum and maximum of $d\bar{f_n}^*(\theta)$ in Eq. A.3 with respect to θ, and then finding values of α that would turn these minima and maxima to zero. This results in the following ranges of α with no contact loss or gain, i.e.

$$\begin{aligned} 198.5^\circ < \alpha < 251.5^\circ \quad &\text{(no contact loss)} \\ 18.5^\circ < \alpha < 63.5^\circ \quad &\text{(no contact gain)} \end{aligned} \tag{A.4}$$